CONSTRUCTING THE SEG/EAGE 3-D SALT MODEL FOR RAY TRACING USING SOBOLEV SCALAR PRODUCTS

P. Bulant

Department of Geophysics, Faculty of Mathematics and Physics, Charles University, Ke Karlovu 3, 121 16 Praha 2, Czech Republic, e-mail: bulant@seis.karlov.mff.cuni.cz

Received: July 22, 2002; Revised: January 16, 2004; Accepted: February 2, 2004

ABSTRACT

Models of geological structures are very often described by values specified at discrete points. A description much more suitable for ray tracing is the parameterization of the model by smooth functions. Such models may be constructed using the method of minimizing the selected objective function.

The efficiency of ray tracing in the constructed model can be evaluated in terms of the average Lyapunov exponent. The exponent may be approximated by the square root of the corresponding Sobolev norm of the model. Including the Sobolev norm in the selected objective function thus allows models suitable for ray tracing to be constructed.

The method is very briefly reviewed and then it is illustrated by constructing two models, which are suitable for ray tracing, and fit the SEG/EAGE 3-D Salt Model data set.

Keywords: Model specification, smoothing, inversion, ray methods, Sobolev norm, Lyapunov exponent, SEG/EAGE 3-D Salt Model

1. INTRODUCTION

Increasing computer power has enabled the very fast development of many numerical modelling techniques, which help us to extend our understanding of the geological structure of the Earth. The application of each numerical method requires a velocity model, which represents our knowledge of the geological structure, and is suitable for the considered method.

Ray-theory based migration techniques have recently been used very frequently. They require very smooth velocity models, which must be continuous, i.e. the model parameters must be known at any point of the model volume. Models suitable for ray tracing may be composed of several blocks separated by smooth structural interfaces. Across the interfaces, the velocity may be discontinuous, inside the blocks, the velocity should vary continuously. One of the parameterizations, which is very suitable for such models, is parameterization by implicit functions. Models suitable for ray tracing are thus very often described by cubic, bicubic or tricubic splines.

On the other hand, the geological structure is very often described by values of material parameters at specified points, usually gridpoints of dense rectangular grids. Similarly, structural interfaces are frequently represented by sets of points corresponding to the interfaces, usually organized into triangular meshes. The conversion between this kind of model parameterization and the spline parameterization, suitable for ray tracing, is a complex task.

In this paper, we would like to present the method of constructing a B-spline parameterized velocity model, suitable for ray tracing, from the given values of velocity and given coordinates of points at structural interfaces. The method is explained for the example of the construction of the models, which are suitable for ray tracing, and fit the gridded values of velocity and the triangulated structural interfaces of the SEG/EAGE 3-D Salt Model data set. The construction of the models is described step–by–step, and an emphasis is put on the proper selection of the relevant numerical parameters (dimensions of model spline grids and weighting factors of the Sobolev norm).

This paper should extend our knowledge about smoothing effects of the Sobolev norm. We believe, that the knowledge will be applicable also to the travel time inversion, in which the first summand of the objective function will be the model covariance function containing the difference between measured and synthetic travel times (*Klimeš, 2002b*).

2. METHOD OF MODEL CONSTRUCTION

The method described in this paper was proposed by *Klimeš (2000a)*. Its detailed theoretical description has been given by *Bulant et al. (2001)*, and published by *Bulant (2002)*. Numerical examples of using the method can be found in *Klimeš (2000b)*, *Bulant (2000)* and *Žáček (2002)*. In this paper, we shall review the basic ideas of the method which concern the construction of models for ray tracing, and we shall demonstrate them for the example of the construction of the SEG/EAGE 3-D Salt Model. This paper thus gives more technical information to the method described in *Bulant (2002)*, and follows the intermediate steps necessary to obtain the results published in Chapter 4.2 of *Bulant (2002)*.

The SEG/EAGE 3-D Salt Model data set (*Aminzadeh et al., 1997*) contains one file with the values of the P-wave velocity specified at gridpoints of a dense 3-D regular rectangular grid, and several files with triangulated structural interfaces. We refer to the given discrete values of velocity and the given coordinates of points at interfaces as "data".

We take the given data, and fit them with a continuous B-spline parameterized velocity model. The method is as follows: we choose a simple starting parameterization of the model, we form an objective function, and we build the model using the method of minimizing the selected objective function. As this is an inverse problem, we shall speak of the "inversion" of the given data.

The objective function of the inversion is formed by two summands. The first one is the mean–squared difference between the data and the model being constructed. The second summand is the Sobolev norm of the functions parameterizing the model being constructed. Generally, the Sobolev scalar product of two functions is a linear combination of the L_2 Lebesgue scalar products of the zero, first, second or higher derivatives of the functions. The Sobolev norm of the functions is then defined as the square root of the Sobolev scalar product. As proposed by *Klimeš (2000a)*, we use the Sobolev norm composed of the second partial derivatives of the functions parameterizing the model being constructed.

There are two main reasons for including the Sobolev norm in the objective function. Firstly, the Sobolev norm regularizes ill–conditioned inversions, which enables us to control the behaviour of the model functions in regions not illuminated by the data. A typical example of such application is the fitting of structural interfaces for which the data are available only in some parts of the model, see Section 3.5.1.

Secondly, the minimization of the corresponding Sobolev norm during the inversion of the given data allows us to construct a model optimal for the selected computational method, i.e. for ray tracing. *Klimeš (2000a)* demonstrated the selection of Sobolev norms which ensure the accuracy of different numerical methods in the smoothed models. For the ray tracing the situation is more complex. The feasibility and efficiency of ray tracing imposes relatively strong constraints on the smoothness of the velocity models, but, unfortunately, we still have no quantitative criteria of applicability and accuracy of ray methods or their extensions. Instead, we use the criterion of the numerical efficiency of ray tracing, based on the numbers of arrivals calculated in the model.

In complex models, the behaviour of rays becomes chaotic and geometrical spreading, density of caustic surfaces and number of arrivals increase exponentially with the travel time. The exponential increment may be quantitatively described in terms of the "average Lyapunov exponent" of ray tracing in the model, introduced by *Klimeš (2000c,2002a)*. The average Lyapunov exponent may roughly be approximated by the square root of the Sobolev norm composed of the second partial derivatives of the functions describing the velocity field in the model (*Klimeš, 2000a*). This enables us to determine the quantitative criteria on models, so that they are suitable for ray tracing, in terms of Sobolev scalar products.

We choose the maximum average Lyapunov exponent for the model, we estimate the maximum Sobolev norm of the model, and we estimate the value of weighting factor S_u of the Sobolev norm. We then perform the inversion, compute the values of the average Lyapunov exponent and the Sobolev norm in the inverted model, re-estimate the value of S_u, and continue iteratively with the inversion until we obtain a model with the required smoothness. We may thus construct models in which ray tracing will be possible and numerically efficient. We remind the reader that we cannot infer about the applicability and accuracy of ray tracing in the models.

3. CONSTRUCTING THE SEG/EAGE 3-D SALT MODEL FOR KIRCHHOFF MIGRATIONS

Routines for application of the above described minimization of the Sobolev norm during the model building inversion have been coded and incorporated in the existing Fortran 77 package **MODEL**, which serves to specify heterogeneous seismic models composed of smooth blocks with arbitrary varying seismic parameters. For the description of the basic ideas of the model specification refer to *Červený et al. (1988)*, the latest version of the package may be found at http://sw3d.mff.cuni.cz . All the computations are carried out on a PC Pentium with 64 Mbytes of memory.

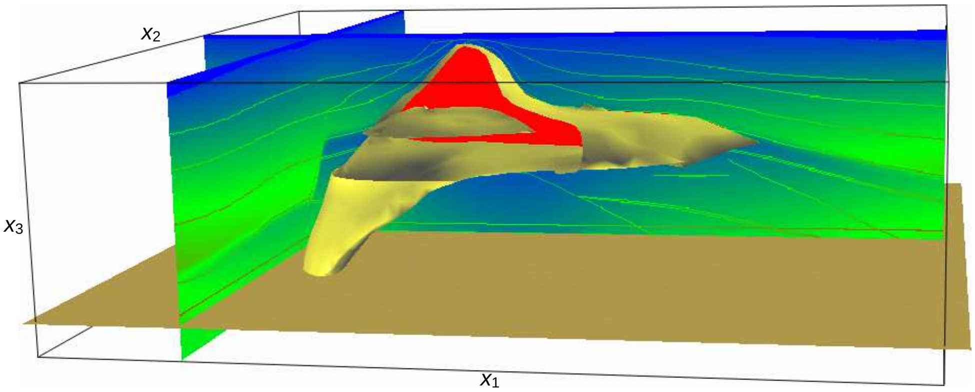

Fig. 1. **GOCAD** snapshot of the salt interface, the bottom flat interface, and two velocity sections through the SEG/EAGE 3-D Salt Model. The horizontal dimensions of the model are 13.5 km times 13.5 km, its vertical dimension is 4.2 km. The surfaces corresponding to the salt interface are yellow, the bottom flat interface is brown. The colour scale of the velocity sections ranges from dark blue for 1500 $\mathrm{m\,s^{-1}}$ in the water to red for 4450 $\mathrm{m\,s^{-1}}$ in the salt body.

The SEG/EAGE 3-D Salt Model (*Aminzadeh et al., 1997*), see Fig. 1, is specified in a form suitable for the **GOCAD** modelling software. Several interfaces in the model are stored in the form of triangulated surfaces, and the 3-D P-wave velocity cube is given. From the point of view of ray tracing, the gridded velocities and the points at the interfaces are not a complete model, because the values of the material parameters must be known at each point of the model volume for ray tracing. Ray tracing also requires much smoother models than in the case of SEG/EAGE 3-D Salt Model data set. The dominant wavelength should be much smaller than the scale of the model variations. For example the shape of the interface limiting the salt body is obviously too complex, see Fig. 2, and the interface must be smoothed, see Fig. 3. Moreover, model specification for ray tracing should be much more effective to enable efficient and fast calculations; the extent of the files with models suitable for ray tracing is usually in tens of kilobytes, while the extent of the file with the velocity cube of the SEG/EAGE Salt Model data set is more than 380 megabytes.

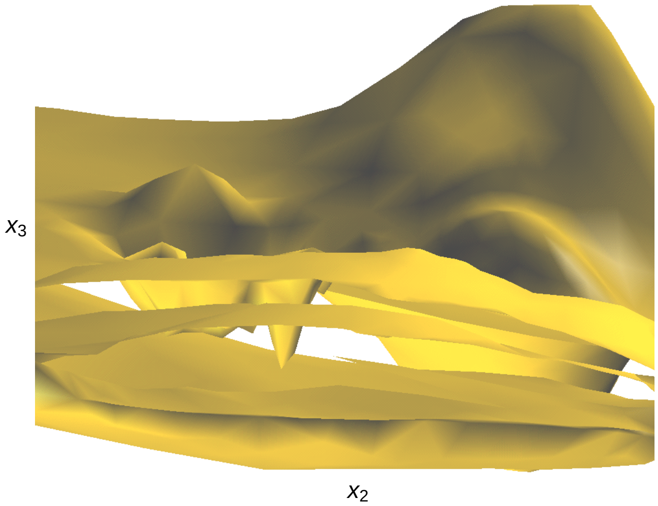

Fig. 2. Detailed GOCAD snapshot of the triangulated surface of the salt in the SEG/EAGE 3-D Salt Model data set. The surface is discontinuous and displays a very complex geometry.

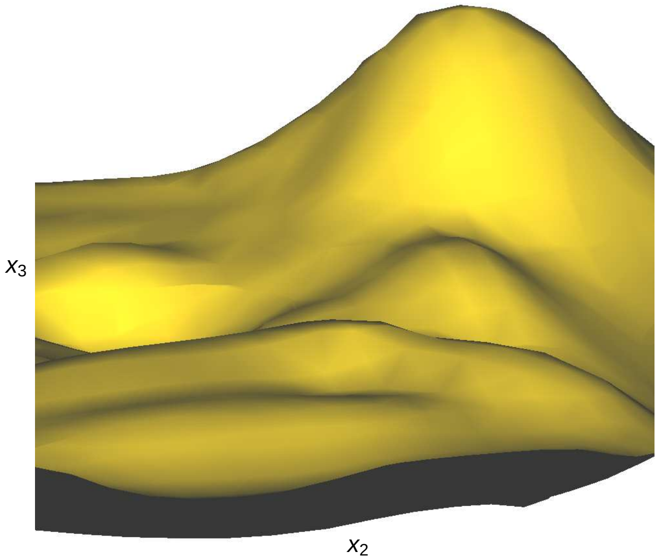

Fig. 3. Detailed GOCAD snapshot of the salt interface in the resulting model obtained after the inversion. The surface is continuous and much smoother than the original triangulated surface shown in Fig. 2.

In the first example, we shall construct a smooth one–block model without interfaces, and in the second example a model containing the salt body and some other selected interfaces.

3.1. Data for the model

The dimensions of the model are 13.5 km times 13.5 km times 4.2 kilometres. The P-wave velocity is discretized on a grid of $676 \times 676 \times 210$ points with a spacing of $20 \times 20 \times 20\,\mathrm{m}^3$. This is a very large amount of data, and we immediately see that a much sparser grid must be used for the data for the inversion. We thus resample the velocities to the grid with the spacing $40 \times 40 \times 40\,\mathrm{m}^3$, which fits into the 64 Mbytes of memory available on our PC. On this grid we invert the velocity into slowness. On the slowness grid we decided to perform arithmetic averaging and we calculate slownesses on the individual sparser grids of different dimensions which are then used as the data for the inversion. We have decided to average the slownesses as the data for the inversion rather than the velocities, because, as it is well known, in the homogeneous material the averaging of the slownesses preserves the ray travel times, and is thus generally considered to work better than the averaging of the velocities. The advantage of the grids obtained by averaging is that their gridpoints need not coincide with the gridpoints of the original grid, and their gridspacing may thus be arbitrary.

3.2. The grid for the calculation of the velocity deviations and the model spline grids

To estimate the error of the model building inversion, we calculate the velocity deviations of the data from the constructed model. The calculation of the deviations on the full $20 \times 20 \times 20\,\mathrm{m}^3$ grid is very time consuming. We thus looked for a sparser grid, which would speed up the calculation, providing approximately the same results as the full grid. We decided to use the grid with the spacing $60 \times 60 \times 20\,\mathrm{m}^3$ for the calculation of the deviations.

The structural interfaces in the model and the 3-D slowness fields in individual model blocks are modelled by tricubic B–splines, which are defined by the values specified at the gridpoints of the model spline grids. The dimensions and the coordinates of the gridpoints of the spline grids are selected manually before the inversion. The model spline grids may be irregular and need not cover the whole model volume. The values at the gridpoints are then calculated during the inversion. The number M of model parameters thus corresponds to the dimensions of the model spline grids. Due to the limited computer memory, the dimensions of the model spline grids must be chosen carefully.

3.3. Choosing the maximum Lyapunov exponent and the maximum Sobolev norm

As mentioned in Section 2, our criterion of suitability of the constructed model for ray tracing is the average Lyapunov exponent $\bar{\lambda}$ of the model. We choose the maximum average Lyapunov exponent $\bar{\lambda}_{\max}$ according to Eq.(11) of *Bulant (2002)*, which reads

$$\bar{\lambda} \leq \frac{2}{T_{\mathrm{max}}} \quad , \tag{1}$$

where $T_{\mathrm{max}} \geq T_{\mathrm{S}} + T_{\mathrm{R}}$ is the maximum sum of travel times from the source and from the receiver. To estimate T_{max}, we compute the average slowness of the data $\langle u \rangle = 0.428\ 10^{-3}\,\mathrm{s\,m^{-1}}$. If we consider the maximum sum of the ray paths to be about 14500 m, we arrive at the estimation that the sum $T_{\mathrm{S}} + T_{\mathrm{R}}$ is limited by $T_{\mathrm{max}} = 6.21$ sec. We thus choose the maximum average Lyapunov exponent $\bar{\lambda}_{\mathrm{max}}$ of the model as

$$\bar{\lambda}_{\mathrm{max}} = \frac{2}{T_{\mathrm{max}}} = 0.322\,\mathrm{s^{-1}} \quad . \tag{2}$$

The maximum Sobolev norm $\|u\|_{\mathrm{max}}$ of the slowness field in the model chosen according to Eq.(13) of *Bulant (2002)* is $\|u\|_{\mathrm{max}} = 0.152\ 10^{-9}\,\mathrm{s\,m^{-3}}$.

The theory of average Lyapunov exponents has recently been developed only for models without interfaces. We still have no quantitative criteria for the smoothness of the structural interfaces, and we thus first try to apply the minimum reasonable smoothing of the interfaces. Whether the interfaces are sufficiently smooth will be tested by ray tracing.

3.4. One–block version of the Salt Model

We try to fit the data by a smooth model, composed of one block with three–dimensionally varying velocity. The data for the inversion are the slownesses on a coarser grid, as mentioned in Section 3.1. In the model, we are interpolating the slowness by tricubic B-splines. The inversion is linear, with objective function

$$y = \left(\frac{|u - u_0|}{\sigma_u} \right)^2 + (S_u \|u\|)^2 \quad , \tag{3}$$

where $|u - u_0|$ is the standard slowness deviation of the model from the gridded slownesses, $\sigma_u = 1\,\mathrm{s\,m^{-1}}$ is the given unit slowness deviation, and S_u is the weighting factor of the 3-D Sobolev norm $\|u\|$ of the slowness field in the model.

We first perform the inversion with $S_u = 0\,\mathrm{m^3\,s^{-1}}$ (i.e. without smoothing), and search for the best model parameterization, which would yield the lowest standard relative velocity deviation $|\frac{v - v_0}{v_0}|$ of the velocity in the model from the velocity in the data cube. We start with slowness data grid intervals of $500 \times 500 \times 500\,\mathrm{m^3}$ and model B-spline intervals of $1000 \times 1000 \times 1000\,\mathrm{m^3}$. We then try denser and sparser spline grids, keeping in mind that the parameterization must not be denser than the data, and considering the memory requirements of the method. (The requirements of the current coding of the method are $M(D + M)$ storage locations, where M is the number of model parameters, and D is the number of data points.) We find that the spline grid should be densified vertically, and that the data grid may be sparser horizontally, see Table 1.

Table 1. Results of the inversion of the slowness field in the Salt Model without smoothing.

$\frac{\text{number of data gridpoints}}{\text{data grid intervals / m}^3}$	$\frac{\text{number of model spline points}}{\text{model spline intervals / m}^3}$	$\lvert\frac{v-v_0}{v_0}\rvert/(\%)$	$\lVert u\rVert/(\mathrm{s\,m^{-3}})$	$\bar{\lambda}/(\mathrm{s^{-1}})$
$\frac{28\times28\times9}{500\times500\times500}$	$\frac{15\times15\times5}{1000\times1000\times1000}$	9.50	$0.172\ 10^{-9}$	0.260
$\frac{28\times28\times9}{500\times500\times500}$	$\frac{9\times15\times5}{1750\times1000\times1000}$	9.68	$0.155\ 10^{-9}$	0.250
$\frac{28\times28\times9}{500\times500\times500}$	$\frac{24\times15\times5}{600\times1000\times1000}$	9.47	$0.185\ 10^{-9}$	0.264
$\frac{28\times28\times9}{500\times500\times500}$	$\frac{15\times15\times8}{1000\times1000\times500}$	7.80	$0.378\ 10^{-9}$	0.298
$\frac{23\times23\times11}{600\times600\times400}$	$\frac{15\times15\times5}{1000\times1000\times1000}$	9.48	$0.174\ 10^{-9}$	0.262
$\frac{23\times23\times11}{600\times600\times400}$	$\frac{15\times15\times9}{1000\times1000\times500}$	7.63	$0.480\ 10^{-9}$	0.362
$\frac{18\times18\times17}{800\times800\times250}$	$\frac{15\times15\times9}{1000\times1000\times500}$	7.54	$0.511\ 10^{-9}$	0.374
$\frac{18\times18\times17}{800\times800\times250}$	$\frac{12\times12\times14}{1200\times1200\times300}$	7.13	$0.833\ 10^{-9}$	0.441
$\frac{14\times14\times21}{1000\times1000\times200}$	$\frac{12\times12\times14}{1500\times1500\times250}$	7.29	$1.086\ 10^{-9}$	0.516
desired values			$0.152\ 10^{-9}$	0.322

For the best model parameterization $\frac{12\times12\times14}{1200\times1200\times300}$ and the data $\frac{18\times18\times17}{800\times800\times250}$ we calculate the standard slowness deviation $|u-u_0| = 0.322\ 10^{-4}\,\mathrm{s\,m^{-1}}$, we estimate

$$S_u = \frac{|u-u_0|}{\sigma_u \lVert u\rVert_{\max}} = \frac{0.322\ 10^{-4}\,\mathrm{s\,m^{-1}}}{1\,\mathrm{s\,m^{-1}}\ 0.152\ 10^{-9}\,\mathrm{s\,m^{-3}}} = 211842\,\mathrm{m^3\,s^{-1}} \quad , \tag{4}$$

and we enter the rounded value of

$$S_u = 200000\,\mathrm{m^3\,s^{-1}} \quad , \tag{5}$$

for the second iteration. We then choose several values of S_u in order to see how sensitive the model is with respect to S_u, see Table 2.

Table 2. Results of the inversion of the slowness field in the Salt Model with respect to weighting factor S_u of the Sobolev norm used.

	$\lvert\frac{v-v_0}{v_0}\rvert/(\%)$	$\lVert u\rVert/(\mathrm{s\,m^{-3}})$	$\bar{\lambda}/(\mathrm{s^{-1}})$
$S_u = 0\,\mathrm{m^3\,s^{-1}}$	7.13	$0.833\ 10^{-9}$	0.441
$S_u = 25000\,\mathrm{m^3\,s^{-1}}$	7.64	$0.400\ 10^{-9}$	0.340
$S_u = 50000\,\mathrm{m^3\,s^{-1}}$	8.22	$0.254\ 10^{-9}$	0.316
$S_u = 100000\,\mathrm{m^3\,s^{-1}}$	9.02	$0.153\ 10^{-9}$	0.263
$S_u = 200000\,\mathrm{m^3\,s^{-1}}$	9.85	$0.091\ 10^{-9}$	0.224
desired values		$0.152\ 10^{-9}$	0.322

We consider the model obtained after the inversion with the value of $S_u = 50000\,\mathrm{m^3\,s^{-1}}$ as the best smooth one–block model, which meets our requirements.

3.5. Salt Model – version with interfaces

We try to fit the data with a model containing the most important interfaces, which are characterized by the highest discontinuities in the velocity field. These interfaces are the ocean bottom, the interface confining the salt body, the geopressure horizon, and the bottom flat interface. Concerning the velocity field, we use the slownesses on the coarser grid as the data, and we interpolate the slowness by tricubic B-splines in the model. The inversion is again linear with objective function

$$y = \left(\frac{|x - x_0|}{\sigma_x} \right)^2 + (S_x \|x\|)^2 + \left(\frac{|u - u_0|}{\sigma_u} \right)^2 + (S_u \|u\|)^2 \quad , \tag{6}$$

where $|x - x_0|$ is the standard deviation of the position of the interfaces in the constructed model from the triangulated interfaces in the original data set, $\sigma_x = 1\,\mathrm{m}$ is the given unit interface deviation, $\|x\|$ is the 3-D Sobolev norm of the curvature of the interfaces in the constructed model, and S_x is the numerical parameter which controls the smoothing of the interfaces during the inversion.

The inversion of the interfaces and the inversion of the slowness field are mutually independent. We can thus perform the inversion of the interfaces in the first step, and the inversion of the slowness in the second step. This fact is of great importance, because to invert the slowness we must know the block of the model, in which the gridpoint is located, for each data gridpoint. This information may be computed after inverting the interfaces, and we are then able to invert the velocities.

3.5.1. Inversion of the interfaces

For all the interfaces, except the salt interface, we may use the triangulated surfaces in the GOCAD representation as the data for inversion. In case of the salt interface, the corresponding GOCAD file containing all the triangles of the interface is discontinuous. In the data set the discontinuities are filled by triangulated surfaces called faults, but the faults not only fill the discontinuities, but they continue to quite a long distance from the surface of the salt. We tried to model the interface as one surface, but all our attempts failed, and so the salt interface must be fitted as two surfaces. We thus generate two files according to the discontinuity in the velocity cube corresponding to the surface of the salt body: one file with the points at the top of the salt, and one with the points at the bottom of the salt. We now have 601 data points for the ocean bottom, 1780 points for the geopressure horizon, and 4 points for the bottom flat interface from the GOCAD files, and we have 6425 points for the salt top and 6336 data points for the salt bottom obtained from the discontinuity in the velocity cube.

We choose the starting parameterization of the interfaces manually, taking a constant function for the flat interface, regular spline grids for the ocean bottom and for the geopressure horizon, and irregular spline grids for the salt surfaces with 18 times 19 points regularly spaced in the region covered by the data, and with the outer spline points at the sides of the model. The outer points enable us to control the behaviour of the functions describing the salt interfaces in the parts of the model not covered by the data for the salt. We first perform the inversion of the interfaces with $S_x = 0\,\mathrm{m}$, i.e. with interfaces smoothed just by the projection onto the B-splines. We obtain oscillations of both salt surfaces outside the region covered by the data for the salt. The oscillations produce several spurious salt bodies around the salt body given by the data. In the next step of the inversion we thus include the minimization of the curvature of the interfaces by increasing the value of S_x until the spurious salt bodies disappear, and we reach a minimum reasonable smoothing of the interfaces, characterized by acceptable values of standard interface deviations. We also optimize the dimensions and the position of the gridpoints of the B-spline grids for the interfaces.

Finally, the bottom interface is modelled by the constant function, the ocean bottom is parameterized by 6 times 6 spline points spaced at 2800 metres, the geopressure horizon is parameterized by 8 times 8 points spaced at 2000 metres, both the top and the bottom of the salt are parameterized by 20 times 21 points spaced at 400 metres in the salt region. Note, that we have enough data to densify the parameterization of the geopressure horizon and of the salt interfaces, but we are constrained by the limited computer memory.

Another possibility for the inversion of the interfaces is to split the **GOCAD** file with all the points of the salt interface into two files, one with 990 points for the top of the salt, and the second with 577 points for the bottom of the salt. We may now densify the parameterization of the geopressure horizon to 29 times 29 points spaced at 500 metres, the parameterization of the salt bottom may be densified to 24 times 23 points spaced at 350 metres, and the parameterization of the salt top may be densified to 32 times 31 points spaced at 250 metres. The root mean square of the error in the position of the geopressure horizon then decreases from 72 m to 9 m, from 63 m to 43 m for the salt top, and from 31 m to 23 m for the salt bottom, but the standard relative deviation of the velocity field in the model increases compared to the model obtained by inverting the data points at interfaces obtained from the velocity cube, see Table 3. This fact is probably caused by the very wide discontinuities in the original triangulated surface of the salt, which are clearly visible in Fig. 1. Using the data from the **GOCAD** file thus probably improves the position of the interface in the regions covered by the data, which causes the decrease of the error in the position of the interfaces, which is calculated at the original data points. On the other hand, the wide discontinuities in the **GOCAD** file probably cause the mispositioning of the interface in the region of the discontinuities and the increase of the error in the velocity field.

Table 3. Results of the inversion in the Salt Model in dependence on the data used for the salt interface and in dependence on the parameterization of the geopressure horizon and of the salt surfaces. The velocity is described by the same functions in all the four models. The lowest velocity deviation is obtained for the salt interface modeled using the data obtained from the discontinuity in the velocity field.

	$\frac{\|u\|}{(\mathrm{s\,m^{-3}\,10^{-9}})}$	$\frac{\left\|\frac{v-v_0}{v_0}\right\|}{(\%)}$	$\frac{\left\|\frac{u-u_0}{u_0}\right\|}{(\%)}$	$\frac{\|v-v_0\|}{(\mathrm{m\,s^{-1}})}$	$\frac{\|u-u_0\|}{(\mathrm{s\,m^{-1}\,10^{-4}})}$
data from velocity field	0.199	5.53	5.86	143	0.208
data from **GOCAD** files	0.199	6.64	6.62	168	0.229
data from **GOCAD** files, gp2 densified	0.199	6.57	6.57	167	0.226
data from **GOCAD** files, salt densified	0.199	6.34	6.52	162	0.224

3.5.2. Inversion of the slowness field

The first test is analogous to the slowness inversion in the one–block model. As the data, we again use slownesses computed by arithmetical averaging. In the model blocks corresponding to the background, we are again interpolating the slowness using tricubic B-splines. Inside the block representing the salt, the slowness is constant.

We start the slowness inversion with the value $S_u = 0\,\mathrm{m}^3\mathrm{s}^{-1}$ and a manually selected parameterization of the slowness field, and we search for the best combination of data grid and B-spline grids for the slowness outside the salt body. We then include the smoothing of the slowness field and we examine the behaviour of the model with respect to S_u. Due to the limited computer memory, we must use a data grid as sparse as possible, in order to be able to densify the model parameterization. On the other hand, the data grid must always be denser than the model parameterization.

We start with the data grid of $68 \times 68 \times 20$ points spaced at $200 \times 200 \times 200\,\mathrm{m}^3$. Table 4 demonstrates that the data may be sparser horizontally, but should be densified vertically.

The results also show that for relatively small values of weight S_u the relative velocity deviation may decrease with increasing value of S_u. This usually happens when the number of data points is not sufficiently higher than the number of spline points. If in such a case the inversion with $S_u = 0\,\mathrm{m}^3\mathrm{s}^{-1}$ is possible, it yields a slowness field displaying random oscillations. Increasing S_u then removes the random oscillations, regularizes the slowness field, and the velocity deviation decreases. A further increase of S_u then means smoothing and causes an increase in the deviation. See also Table 6.

Table 4. Results of the inversion in the Salt Model with respect to the grid dimensions of the data used for the P-wave slowness and with respect to the parameterization of the slowness field in the model. The interfaces are described by the same functions in all the models.

data grid / data grid intervals	model spline grid / model spline intervals	S_u / $\mathrm{m}^3\mathrm{s}^{-1}$	$\lVert u\rVert$ ($\mathrm{s\,m}^{-3}\ 10^{-9}$)	$\lvert\frac{v-v_0}{v_0}\rvert$ (%)	$\lvert\frac{u-u_0}{u_0}\rvert$ (%)	$\lvert v-v_0\rvert$ ($\mathrm{m\,s}^{-1}$)	$\lvert u-u_0\rvert$ ($\mathrm{s\,m}^{-1}\ 10^{-4}$)
68×68×20 / 200×200×200	5×5×3 / 3500×3500×∼1700	0	0.183	5.53	6.13	146	0.213
46×46×14 / 300×300×300	5×5×3 / 3500×3500×∼1700	0	0.165	5.74	6.34	151	0.223
34×34×20 / 400×400×200	5×5×3 / 3500×3500×∼1700	0	0.183	5.51	6.08	145	0.212
23×23×20 / 600×600×200	5×5×3 / 3500×3500×∼1700	0	0.190	5.59	6.19	147	0.216
17×17×20 / 800×800×200	5×5×3 / 3500×3500×∼1700	0	0.195	5.66	6.27	149	0.219
11×11×20 / 1340×1340×200	5×5×3 / 3500×3500×∼1700	0	0.177	5.63	6.30	148	0.220
17×17×20 / 800×800×200	8×8×9/8 / 2000×2000×250	10000	0.294	5.45	5.83	143	0.203
17×17×39 / 800×800×100	8×8×9/8 / 2000×2000×250	10000	0.257	5.24	5.69	137	0.196
11×11×20 / 1340×1340×200	8×8×9/8 / 2000×2000×250	10000	0.363	5.63	6.96	146	0.211
11×11×20 / 1340×1340×200	10×10×10/9 / 1500×1500×220	10000	0.468	6.03	6.17	155	0.223
11×11×20 / 1340×1340×200	10×10×10/9 / 1500×1500×220	25000	0.199	5.53	5.86	143	0.208

To examine the effect of the slowness averaging, another test has been done with the slownesses used as the data for the slowness inversion in a model parameterized by $5 \times 5 \times 3$ points spaced at $3500 \times 3500 \times \sim 1700\,\mathrm{m}^3$. Four kinds of data have been prepared on the grid of $68 \times 68 \times 20$ points spaced at $200 \times 200 \times 200\,\mathrm{m}^3$. First, the values of velocity on the grid $200 \times 200 \times 200\,\mathrm{m}^3$ were chosen from the original dense grid and inverted (as $u = 1/v$) into slowness values. We call this data "chosen". Second, the values of velocity were chosen on the grid $40 \times 40 \times 40\,\mathrm{m}^3$, inverted into slowness values, and the slowness on the grid $200 \times 200 \times 200\,\mathrm{m}^3$ was computed by arithmetical averaging from the slowness on the $40 \times 40 \times 40\,\mathrm{m}^3$ grid, analogously as the data for the one–block version of the Salt Model. We call this data "averaged". The third kind of data is similar to the first, but the artificial thin layers, modelled by the velocity step of 15 % and serving as reflectors for migrations (*Aminzadeh et al., 1997*), were removed from the slowness field. The fourth kind of data is similar to the second kind, again without the artificial thin layers. The results of the test, shown in Table 5, demonstrate that the "chosen" slownesses provide better results than the "averaged" slownesses, and that the removal of the artificial thin layers improves the results of the inversion.

If the data for the inversion represent a smooth function to be modelled, and if they do not contain any noise, it is much better to use the "chosen" data than the "averaged" data. For example, if we imagine a smooth one–dimensional function represented by a set of points, the "chosen" points always represent the functional values, but the "averaged" points are shifted from the functional values in the direction of the second derivatives. The artificial thin layers in the Salt Model may thus be understood as the noise of the smooth velocity function, and the best results are obtained if we remove this noise and if we use the "chosen" slowness data instead of the "averaged" slowness data.

Note that here the "chosen" data work much better than the "averaged" data mainly because the "averaged" data transfer the information about the velocity inside the salt into the background velocity field. In the one–block version of the model the difference between the "chosen" and the "averaged" data is not so significant, and we can keep the "averaged" data which are advantageous for their arbitrary grid spacing.

Table 5. Results of the inversion in the Salt Model in dependence on the kind of data used for the slowness inversion. For the description of the kinds of data see the text.

	$\frac{S_u}{\mathrm{m}^3\mathrm{s}^{-1}}$	$\frac{\Vert u \Vert}{(\mathrm{s\,m}^{-3}\ 10^{-9})}$	$\frac{\lvert\frac{v-v_0}{v_0}\rvert}{(\%)}$	$\frac{\lvert\frac{u-u_0}{u_0}\rvert}{(\%)}$	$\frac{\lvert v-v_0\rvert}{(\mathrm{m\,s}^{-1})}$	$\frac{\lvert u-u_0\rvert}{(\mathrm{s\,m}^{-1}\ 10^{-4})}$
slowness chosen	0	0.183	5.53	6.13	146	0.213
slowness averaged	0	0.204	7.04	7.96	182	0.296
slowness chosen, no layers	0	0.190	5.38	5.99	142	0.207
slowness averaged, no layers	0	0.180	6.71	7.65	176	0.280

We have finally decided to use the "chosen" data without the thin layers, we have selected the best combination of the data and of the model parameterization, we have estimated the value of S_u according to Eq.(4), and we have performed the inversion for several values close to the estimated value of S_u, see Table 6. The best model we obtained has the standard relative deviation of velocity $|\frac{v-v_0}{v_0}| = 5.11\%$. The Sobolev norm of the slowness field in the model is $0.302\ 10^{-9}\,\mathrm{s\,m^{-3}}$. The average Lyapunov exponent of the velocity field in the model is $0.152\,\mathrm{s^{-1}}$. Note that the exponent does not take into account the discontinuities in the velocity field across the structural interfaces.

Let us also note that the standard relative velocity deviation of 5.11% does not imply relative error of 5.11% in ray travel times, because the rays will probably propagate through both areas of positive and of negative velocity deviation. We remind the reader that we are not able to calculate travel time deviations, because we cannot perform ray tracing in the original discrete velocity grid.

Table 6. Results of the inversion in the Salt Model with respect to weighting factor S_u. The slowness in the model is parameterized by $8\times8\times9$ points spaced at $2000\times2000\times250\,\mathrm{m^3}$. The values of slowness on the grid of $17\times17\times39$ points spaced at $800\times800\times100\,\mathrm{m^3}$, calculated from the velocity chosen from the original dense grid with removed artificial thin layers, are used as the data for the inversion.

$\frac{S_u}{\mathrm{m^3\,s^{-1}}}$	$\frac{\lVert u\rVert}{(\mathrm{s\,m^{-3}}\ 10^{-9})}$	$\frac{\lvert\frac{v-v_0}{v_0}\rvert}{(\%)}$	$\frac{\lvert\frac{u-u_0}{u_0}\rvert}{(\%)}$	$\frac{\lvert v-v_0\rvert}{(\mathrm{m\,s^{-1}})}$	$\frac{\lvert u-u_0\rvert}{(\mathrm{s\,m^{-1}}\ 10^{-4})}$	$\frac{\bar{\lambda}}{(\mathrm{s^{-1}})}$
2500	0.374	5.15	5.75	137	0.197	0.181
5000	0.302	5.11	5.70	136	0.195	0.152
7500	0.256	5.11	5.70	136	0.195	0.133
10000	0.222	5.12	5.70	136	0.195	0.121

3.6. Tests of ray tracing in the inverted models

We performed several tests of ray tracing in the models obtained after the inversions. As it is difficult to display the results of 3-D ray tracing clearly, we decided to shoot the rays only in the direction of the x_1-x_3 plane (one–parametric shooting in a 3-D model). We then projected the computed rays onto the x_1-x_3 plane and onto the x_2-x_3 plane. The projected rays together with the velocity sections corresponding to the x_2 coordinates of the sources are displayed in Figs. 4 and 5.

3.7. Comparison with other smoothing methods

We compare the described smoothing method with four other methods. The first one is the simple smoothing by the projection onto the B-splines. The second one is arithmetical averaging and the third one is r.m.s. averaging of the slowness. The fourth method is the method of Damped Least Squares (DLS) used in public domain program smooth3d (*Liu, 1994*), which is a part of the package Seismic Un*x developed at Colorado School of Mines, see http://www.cwp.mines.edu/cwpcodes .

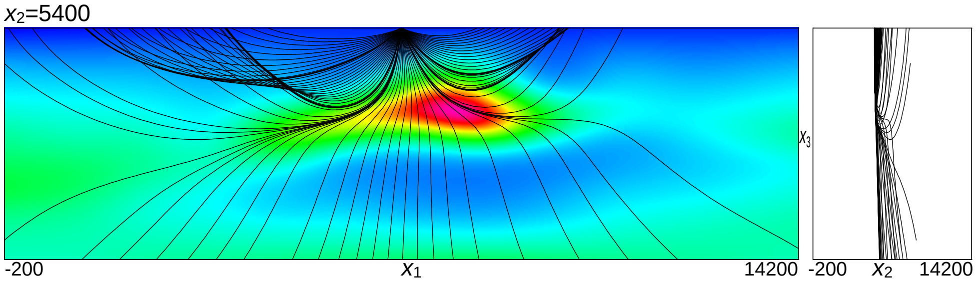

Fig. 4. Rays computed by one–parametric shooting of a refracted wave in the x_1-x_3 plane in the one–block version of the Salt Model. The rays are projected onto the x_1-x_3 and onto the x_2-x_3 planes. The coordinates of the point source are [7000,5400,0] m. The x_1-x_3 plane is coloured according to the P-wave velocity in the x_1-x_3 section containing the point source. The colour scale ranges from dark blue for 1500 $\mathrm{m\,s^{-1}}$ in the water to red for 4450 $\mathrm{m\,s^{-1}}$ in the salt body. The horizontal extents of both the x_1-x_3 and x_2-x_3 sections are 14400 m, the vertical extents of the sections are 4200 m. The reader is reminded that the standard relative deviation of the velocity in the model from the data is 8.22%, and the value of average Lyapunov exponent of the model is $0.316\,\mathrm{s^{-1}}$.

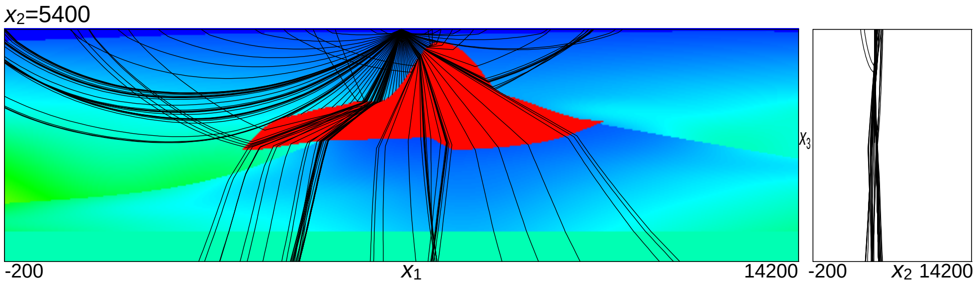

Fig. 5. Rays computed in the Salt Model, the version with interfaces. The initial conditions for the rays and the colour scale of the velocity section are the same as in Fig. 4. The reader is reminded that the standard relative deviation of the velocity in the model from the data is 5.11%, and the value of average Lyapunov exponent is $0.152\,\mathrm{s^{-1}}$.

We apply the methods to the original P-wave velocity data set and create one–block versions of the Salt Model. We try to apply such amount of smoothing, so that we obtain models with standard relative velocity deviation similar to that of our model (8.22%). We then compare the smoothness of the models in terms of the average Lyapunov exponents. We include also comparison of ray tracing in the one–block version of the Salt model smoothed by our method and in the models smoothed by other methods, see Figs. 6 to 10.

The first method is very straightforward. We choose the B-spline grid, in the nodes take the values "chosen" (see Section 3.5.2) from the original P-wave velocity grid, and between the nodes interpolate by the splines. Note that the method is equivalent to our inversion method applied to "chosen" data with zero weighting factor of the Sobolev norm S_u. When we choose the B-spline spacing of $20 \times 20 \times 20\,\mathrm{m^3}$, the relative deviation is 0%. The wider the spacing, the larger the deviation. For example for the spacing of $60 \times 60 \times 20\,\mathrm{m^3}$ we obtain the model with relative velocity deviation of 2.19%. For the spacing of $800 \times 800 \times 240\,\mathrm{m}^3$, the deviation is 8.18%, which is similar to the model obtained by our method. See Fig. 7.

The second method is similar to the first one, but we use the "averaged" (see Section 3.5.2) data. The method is again equivalent to our inversion method applied to "averaged" data with zero weighting factor of the Sobolev norm $S_u = 0$. For the spacing of $1700 \times 1700 \times 400\,\mathrm{m}^3$, we obtain the model with the standard deviation of 8.18%. See Fig. 8.

The third method is almost same as the second method, but we apply root mean square (r.m.s.) averaging of the slowness instead of the arithmetical averaging. The results are about the same as for the second method, see Fig. 9.

The DLS smoothing method is considered to be suitable for smoothing the velocity fields for ray methods (*Liu, 1994*). A smooth velocity function is sought that minimizes the sum of the deviation between the smooth and original velocities, and of the first, second and third derivatives of the velocity. The method is thus similar to our method, the main difference is that DLS is forward technique, while our method is inverse technique. There is also the difference in the Sobolev norm being used: we use the norm composed of second velocity derivatives, the DLS method minimizes first and third derivatives in addition. The numerical realization of the DLS method, program smooth3d, reads the gridded velocities, user chooses the value of smoothing parameter, and obtains the smoothed velocity grid on output. The dimensions of the input and output grids are the same. As we need the velocity to be specified in any point of the model volume, we decided to combine the DLS smoothing with the splines. We choose very dense spline grid of $60 \times 60 \times 20\,\mathrm{m}^3$, and in their nodes we take the values "chosen" from the velocity grid smoothed by DLS. We can assume that the 2.19% of the velocity deviation is thus caused by splines, and the rest by the selected value of the smoothing operator. The larger the operator, the smoother the model, and the larger the velocity deviation. For the value of 1000 of the smoothing operator, the velocity deviation is 8.28%.

We can also construct models with sparser spline spacing and in the spline nodes we can take the values "chosen" from the velocity grid smoothed by DLS with the value of 1000 of the smoothing operator. The model with spline spacing of $800 \times 800 \times 240\,\mathrm{m}^3$ has the relative velocity deviation 8.44%. The model with spline spacing of $1200 \times 1200 \times 300\,\mathrm{m}^3$ has the relative velocity deviation 8.78%, see Fig. 10.

We calculate the average Lyapunov exponents in all the models, see Table 7. We can see that the smoothing by the simple projection of the "chosen" data onto B-splines does not yield models suitable for ray tracing. The model obtained by the projection of the "averaged" data onto B-splines is comparable with the model obtained by our inversion method. The results of the DLS method are slightly worse than the models obtained by our inversion method, which provides smoother model for the selected velocity deviation. We see the main advantages of our concept in the possibility to apriori determine the quantitative criteria on the model smoothness, and to obtain the model of required smoothness in several iterations. The advantage is also the possibility to control the model parameters unresolved by the data, to

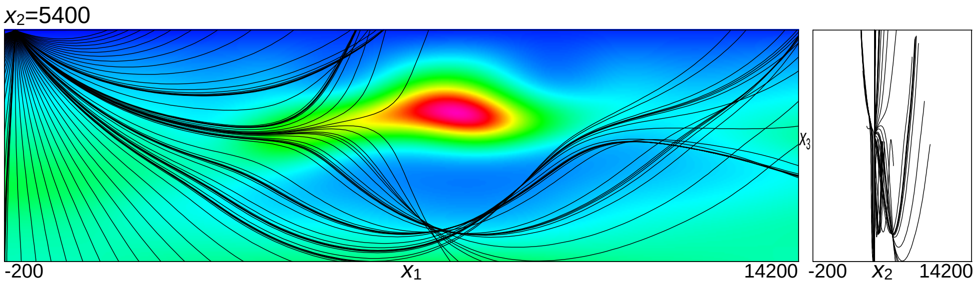

Fig. 6. Rays computed in the one–block version of the Salt Model for the source located at [0,5400,0] m. The remaining initial conditions for the rays and the colour scale of the velocity section are the same as in Fig. 4. The standard relative velocity deviation is 8.22%, and the value of average Lyapunov exponent of the model is $0.316\,\mathrm{s}^{-1}$.

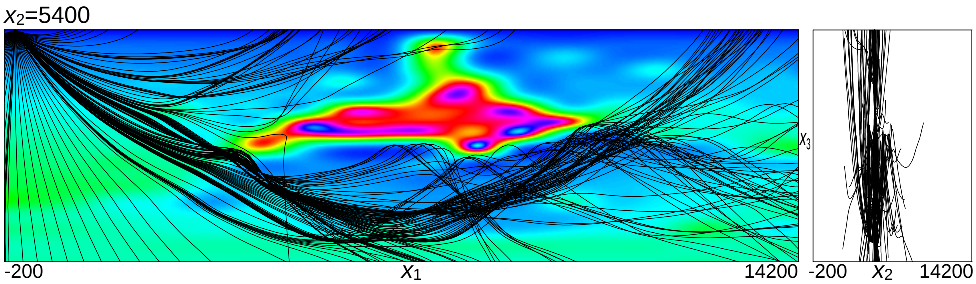

Fig. 7. Rays computed in the one–block version of the Salt Model smoothed by the projection onto B-splines using "chosen" data. The initial conditions for the rays and the colour scale of the velocity section are the same as in Fig. 6. The standard relative velocity deviation is 8.18%, and the value of average Lyapunov exponent is $0.608\,\mathrm{s}^{-1}$.

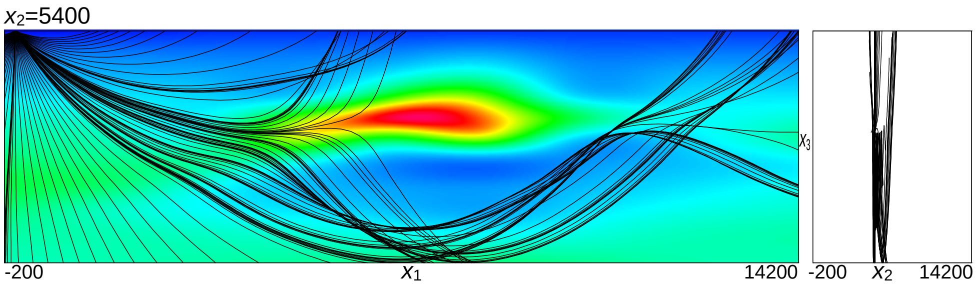

Fig. 8. Rays computed in the one–block version of the Salt Model smoothed by the projection onto B-splines using "averaged" data. The initial conditions for the rays and the colour scale of the velocity section are the same as in Fig. 6. The standard relative velocity deviation is 8.18%, and the value of average Lyapunov exponent is $0.337\,\mathrm{s}^{-1}$.

use irregular data, and to handle structural interfaces in a very similar way as the velocity or slowness fields.

It would be certainly interesting to compare with further smoothing methods. Unfortunately, the author failed to find other widely used methods available in the public domain software.

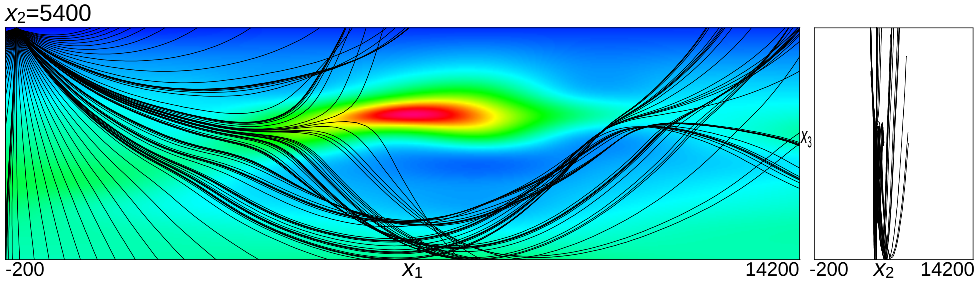

Fig. 9. Rays computed in the one–block version of the Salt Model smoothed by the projection onto B-splines using r.m.s. "averaged" data. The initial conditions for the rays and the colour scale of the velocity section are the same as in Fig. 6. The standard relative velocity deviation is 8.18%, and the value of average Lyapunov exponent is $0.334\,\mathrm{s}^{-1}$.

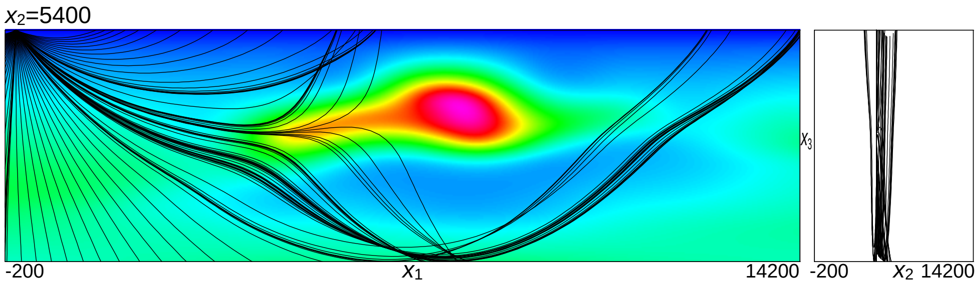

Fig. 10. Rays computed in the one–block version of the Salt Model smoothed by the DLS method. The initial conditions for the rays and the colour scale of the velocity section are the same as in Fig. 6. The standard relative velocity deviation is 8.78%, and the value of average Lyapunov exponent is $0.371\,\mathrm{s}^{-1}$.

Table 7. Standard relative velocity deviation and average Lyapunov exponent of one–block versions of the Salt Model obtained by different smoothing methods. For the description of the models refer to Section 3.7.

short description of the model	$\frac{\text{number of spline points}}{\text{spline intervals / m}^3}$	$\lvert\frac{v-v_0}{v_0}\rvert/(\%)$	$\bar{\lambda}/(\mathrm{s}^{-1})$
model smoothed by inversion	$\frac{12\times12\times14}{1200\times1200\times300}$	8.22	0.316
projection of "chosen" data onto splines	$\frac{17\times17\times18}{800\times800\times240}$	8.18	0.608
projection of "averaged" data onto splines	$\frac{9\times9\times11}{1700\times1700\times400}$	8.18	0.337
projection of r.m.s. "averaged" data onto splines	$\frac{9\times9\times11}{1700\times1700\times400}$	8.18	0.334
smoothing by DLS and projection onto splines	$\frac{226\times226\times210}{60\times60\times20}$	8.28	0.411
smoothing by DLS and projection onto splines	$\frac{17\times17\times18}{800\times800\times240}$	8.44	0.394
smoothing by DLS and projection onto splines	$\frac{12\times12\times14}{1200\times1200\times300}$	8.78	0.363

4. CONCLUSIONS

The geological structure is very often described by discrete values of material parameters, which are usually specified at gridpoints of rectangular grids or at the vertices of triangular meshes. This representation of the model is not suitable for ray tracing, because the ray method requires continuous models. The ray method also imposes relatively strong constraints on the smoothness of the models. Much more suitable is the parameterization of the model by smooth functions. The conversion between the discrete model parameterization and the parameterization by smooth functions may be performed using the method of solving the inverse problem by minimizing the selected objective function.

Including the Sobolev norm in the objective function regularizes an ill-conditioned inversion. It enables the control of the model parameters unresolved by the data being fitted, while the parameters determined by the data remain almost unchanged. The smoothness of the velocity field of the models constructed for the ray methods may be quantitatively described in terms of the average Lyapunov exponent for the model. The average Lyapunov exponent may be approximated by the square root of the corresponding Sobolev norm of the model. This enables us to determine the quantitative criteria on the models, so that they are suitable for ray tracing, in terms of Sobolev scalar products. The criteria then allow us to construct the optimum models of geological structures, in which the numerical efficiency of ray tracing is guaranteed.

The example of inverting the data of the SEG/EAGE 3-D Salt Model data set demonstrates the use of Sobolev norms in building a 3-D model suitable for ray tracing. The method enables a B-spline parameterized model to be created from the given discrete data. It is possible to create the model with or without structural interfaces. The smoothness of the models is simply controlled by the values of the weighting factors of the Sobolev norms. The test of various forms of data for the slowness inversion showed the advantages of using the "averaged" data when constructing a one–block model (see Section 3.7), and of using the "chosen" data for models with interfaces (Section 3.5.2). The tests of ray tracing in the inverted models demonstrate the different behaviour of the rays in the two constructed models, which differ in the presence of the structural interfaces. The basic features of the ray field are similar in both the models. For the selected value of velocity deviation, the method described in this paper provides the smoothest model from all the methods being compared in Section 3.7.

Acknowledgements: The author expresses his thanks to Luděk Klimeš for his kind guidance of the work being presented in the paper. This research has been supported by the Grant Agency of the Czech Republic under Contracts 205/01/0927, 205/04/1104 and 205/01/D097, by the Grant Agency of the Charles University under Contract 237/2001/B-GEO/MFF, by the Ministry of Education of the Czech Republic within Research Project MSM113200004, and by the members of the consortium "Seismic Waves in Complex 3-D Structures", see http://sw3d.mff.cuni.cz .

References

Aminzadeh F., Brac J. and Kunz T., 1997. *3-D Salt and Overthrust Models.* SEG/EAGE 3-D Modeling Series No.1., Soc. Explor. Geophysicists, Tulsa.

Bulant P., 2000. Smoothing 2-D model HESS for Kirchhoff migrations. In: *Seismic Waves in Complex 3-D Structures, Report 10*, pp. 75–82, Dep. Geophys., Charles Univ., Prague, online at http://sw3d.mff.cuni.cz .

Bulant P., 2002. Sobolev scalar products in the construction of velocity models – application to model Hess and to SEG/EAGE Salt Model. *Pure Appl. Geophys.*, **159**, 1487–1506.

Bulant P., Klimeš L. and Žáček K., 2001. Sobolev scalar products in the construction of velocity models. In: *Extended Abstracts of 63rd EAGE Conference (Amsterdam)*, pp. O-24, Eur. Assoc. Geoscientists and Engr., Houten.

Červený V., Klimeš L. and Pšenčík I., 1988. Complete seismic–ray tracing in three–dimensional structures. In: D.J. Doornbos (Ed.), *Seismological Algorithms*, Academic Press, New York, 89–168.

Klimeš L., 2000a. Sobolev scalar products in the construction of velocity models. In: *Seismic Waves in Complex 3-D Structures, Report 10*, pp. 15–40, Dep. Geophys., Charles Univ., Prague, online at http://sw3d.mff.cuni.cz .

Klimeš L., 2000b. Smoothing the Marmousi model for Gaussian–packet migrations. In: *Seismic Waves in Complex 3-D Structures, Report 10*, pp. 63–74, Dep. Geophys., Charles Univ., Prague, online at http://sw3d.mff.cuni.cz .

Klimeš L., 2000c. Lyapunov exponents for 2-D ray tracing without interfaces. In: *Expanded Abstracts of 70th Annual Meeting (Calgary)*, pp. 2293–2296, Soc. Explor. Geophysicists, Tulsa.

Klimeš L., 2002a. Lyapunov exponents for 2-D ray tracing without interfaces. *Pure Appl. Geophys.*, **159**, 1465–1485.

Klimeš L., 2002b. Application of the medium covariance functions to travel–time tomography. *Pure Appl. Geophys.*, **159**, 1791–1810.

Liu Z., 1994. *A velocity smoothing technique based on damped least squares.* CWP-149, Center for Wave Phenomena, Colorado School of Mines, available through http://www.cwp.mines.edu .

Žáček K., 2002. Smoothing the Marmousi model. *Pure Appl. Geophys.*, **159**, 1507–1526.